

## Comparison between the water activation effects by pulsed and sinusoidal helium plasma jets

Han Xu, Dingxin Liu, Wenjie Xia, Chen Chen, Weitao Wang, Zhijie Liu, Xiaohua Wang, and Michael G. Kong

Citation: *Physics of Plasmas* **25**, 013520 (2018);

View online: <https://doi.org/10.1063/1.5016510>

View Table of Contents: <http://aip.scitation.org/toc/php/25/1>

Published by the *American Institute of Physics*

---

---

**COMPLETELY  
REDESIGNED!**



**PHYSICS  
TODAY**

*Physics Today* Buyer's Guide  
Search with a purpose.

# Comparison between the water activation effects by pulsed and sinusoidal helium plasma jets

Han Xu,<sup>1</sup> Dingxin Liu,<sup>1,a)</sup> Wenjie Xia,<sup>1</sup> Chen Chen,<sup>1</sup> Weitao Wang,<sup>1</sup> Zhijie Liu,<sup>1</sup> Xiaohua Wang,<sup>1</sup> and Michael G. Kong<sup>1,2,3</sup>

<sup>1</sup>State Key Laboratory of Electrical Insulation and Power Equipment, Centre for Plasma Biomedicine, Xi'an Jiaotong University, Xi'an 710049, People's Republic of China

<sup>2</sup>Frank Reidy Center for Bioelectronics, Old Dominion University, Norfolk, Virginia 23508, USA

<sup>3</sup>Department of Electrical and Computer Engineering, Old Dominion University, Norfolk, Virginia 23529, USA

(Received 20 November 2017; accepted 5 January 2018; published online 19 January 2018)

Comparisons between pulsed and sinusoidal plasma jets have been extensively reported for the discharge characteristics and gaseous reactive species, but rarely for the aqueous reactive species in water solutions treated by the two types of plasma jets. This motivates us to compare the concentrations of aqueous reactive species induced by a pulsed and a sinusoidal plasma jet, since it is widely reported that these aqueous reactive species play a crucial role in various plasma biomedical applications. Experimental results show that the aqueous  $\text{H}_2\text{O}_2$ ,  $\text{OH}/\text{O}_2^-$ , and  $\text{O}_2^-/\text{ONOO}^-$  induced by the pulsed plasma jet have higher concentrations, and the proportional difference increases with the discharge power. However, the emission intensities of  $\text{OH}(\text{A})$  and  $\text{O}(3\text{p}^5\text{P})$  are higher for the sinusoidal plasma jet, which may be attributed to its higher gas temperature since more water vapor could participate in the plasma. In addition, the efficiency of bacterial inactivation induced by the pulsed plasma jet is higher than that for the sinusoidal plasma jet, in accordance with the concentration relation of aqueous reactive species for the two types of plasma jets. *Published by AIP Publishing.*

<https://doi.org/10.1063/1.5016510>

## I. INTRODUCTION

Cold atmospheric pressure plasmas (CAPs) have been extensively studied in the last decade due to their great potential in diverse application fields such as bacterial inactivation,<sup>1–3</sup> wound healing,<sup>4</sup> dermatology, and cancer therapies,<sup>5–10</sup> as well as food decontamination.<sup>11</sup> In many of these applications, the targets to be treated by plasmas are normally placed in water solutions or humid environments, leading to increasing attention in the research on the interaction between plasma and water. Several research papers have reported that the compositions of reactive species in plasmas—including electrons, ions, UV photons, and the reactive oxygen and nitrogen species (RONS)—are dependent on the type of plasma source and the operation conditions.<sup>12–14</sup> These factors are also crucial for the production of aqueous reactive species when samples are treated by the plasmas; thus, the research on aqueous reactive species induced by different plasmas is of great significance.

As a main production source of atmospheric pressure plasmas, plasma jet has an advantage of delivering a plasma outside the discharge area and, hence, the size of the substrate to be treated is not confined. Plasma jets are normally excited by pulsed voltages with kilohertz repetition frequencies as well as sinusoidal voltages in the kilohertz-to-megahertz range.<sup>15–20</sup> Besides, related studies have been reported with concern of the discharge characteristics,<sup>21</sup> the discharge mechanism,<sup>22,23</sup> and the analysis of plasma products,<sup>24</sup> etc. Recently, the comparisons of pulsed and sinusoidal plasma jets in the gas phase have been reported,<sup>15,25</sup> and the results show that pulsed excitation is more efficient to produce energetic electrons rather than heat the gas,<sup>25</sup> and hence more

reactive species can be generated in pulsed plasmas. From the application point of view, it can be deduced that the pulsed plasma jet has advantages of lower power consumption and higher plasma-chemical efficiency.<sup>26</sup> However, a direct comparison of the water solutions activated by pulsed and sinusoidal plasma jets remains few. There is a report which has found that the sterilization effect in plasma-activated water is better for the pulsed plasma jet,<sup>15</sup> but the underlying mechanism is not well elucidated. Since the plasma-induced aqueous reactive species such as  $\text{ONOOH}$ ,  $\text{O}_3$ , and  $\text{OH}$  are widely thought to be the main antibacterial agents, it is hypothesized that the pulsed plasma jet is more efficient to generate those reactive species in the treated water. The hypothesis needs to be proved by directly comparing the concentrations of aqueous reactive species induced by pulsed and sinusoidal plasma jets with similar parameters, e.g., the discharger power, and the comparison may also provide a better understanding of the production mechanism of aqueous reactive species induced by plasma jets.

In this paper, an experimental study is carried out to directly compare the electrical characteristics, the optical emission spectra, the concentrations of aqueous reactive species, and the bacterial inactivation efficiency for a pulsed plasma jet and its sinusoidal counterpart. Emphasis is made on the correlation of reactive species in gas phase and in liquid phase, with which the production mechanism of aqueous reactive species is discussed.

## II. EXPERIMENTAL METHODS

The schematic diagram of plasma jet source is shown in Fig. 1(a). The high voltage electrode is made of a stainless steel rod, which is sealed in a small quartz capillary with a

<sup>a)</sup>Electronic mail: liudingxin@mail.xjtu.edu.cn

thickness of 0.75 mm. The stainless steel rod and the quartz capillary are placed in the axis of an outer quartz tube, which has an inner and an outer diameter of 4 mm and 6 mm, respectively. The dome tip of the quartz capillary has a distance of 6 mm from the jet nozzle (the nozzle of the outer quartz tube), and helium (99.999% purity) flows through the space between the two coaxial quartz tubes with a rate of 3 SLM. Deionized water treated in the experiments is put in a petri dish with a volume of 2 mL and a thickness of 10 mm. The distance between the plasma jet nozzle and the liquid surface is 7 mm, and there is a copper plate under the petri dish which is used as the ground electrode. As shown in Fig. 1(a), the plasma jet has a needle-plate electrode configuration, and the plasma is found to be very stable for many hours.

In order to directly compare the plasma jets excited by sinusoidal and pulsed voltages, their discharge power and frequency are kept the same at  $P=700$  mW and  $f=8$  kHz. The discharge current and voltage waveforms are shown in Figs. 1(b) and 1(c), along with the discharge images for the two types of plasma jets. The waveforms of discharge voltage and current are recorded by an oscilloscope (Tektronix, DPO3000) with a high-voltage probe (Tektronix, P6015A) and a current probe (Tektronix, P6021). The sinusoidal voltage has a peak-to-peak value of 11.8 kV, while the pulsed voltage has a unipolar peak value of 5.4 kV. The voltage pulse has a width (full width of half maximum) of 1  $\mu$ s, and the rising time and falling time are 30 and 35 ns, respectively. Discharge current peaks at each of the voltage-rising and the voltage-falling edges. It is worth mentioning that the

discharge currents shown in Figs. 1(b) and 1(c) are the total currents which include the component of displacement current. The discharge power is obtained by integrating of the measured voltage and current for each of the plasma jet. As shown in the discharge images, both the plasma plumes for the two types of plasma jets can be in contact with the water surface, but the pulsed plasma plume is slightly wider and brighter than the sinusoidal one, which may be attributed to more reactive species generated by the pulsed excitation with the same discharge power.

The plasma-induced gaseous and aqueous reactive species are measured for comparing the two types of plasma jets. The gaseous reactive species are measured using an optical emission spectrometer (Andor DH720/Shamrock system). The spectral range is from 200 to 800 nm, and for most of the measurements, the grating and the slit width of the spectrometer are set at 1200 g/mm and 200  $\mu$ m, respectively. Moreover, the 309 nm band of OH radical can be used for estimating the gas temperature, and for this purpose, a higher resolution of spectrum is needed with a grating of 2400 g/mm and a slit width of 100  $\mu$ m. The aqueous reactive species are measured using a microplate reader (Thermo Scientific Varioskan<sup>®</sup> Flash Reader) and an electron spin resonance spectrometer (ESR, BrukerBioSpin GmbH, EMX). Chemical fluorescent assays are used to quantitatively measure concentrations of long-lived species including  $\text{H}_2\text{O}_2$  (Amplex<sup>®</sup> Red reagent) and  $\text{NO}_2^-/\text{NO}_3^-$  (Griess reagent). However, no desired signal is detected for nitrate and nitrite, indicating that their concentration is lower than the detection limit of  $\sim 1$   $\mu$ M. Short-lived species are captured by their corresponding spin traps to

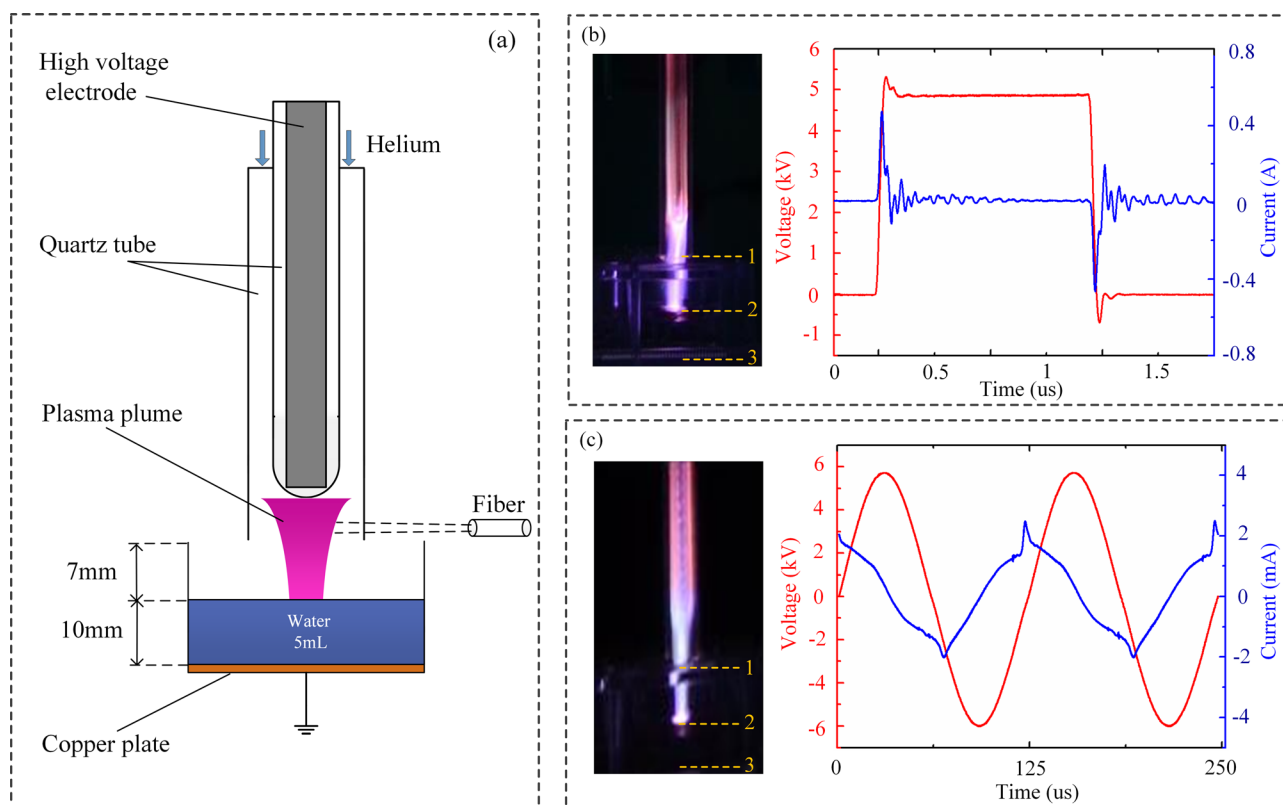


FIG. 1. Schematic diagram of the experimental set-up (a), discharge images and I-V characteristics of the plasma jet excited by a pulsed voltage (b), and a sinusoidal voltage (c). In the discharge images, the numbers 1, 2, and 3 represent the jet nozzle, the liquid surface, and the copper plate, respectively.

accumulate and then be measured by ESR. DMPO (5,5-dimethyl-1-pyrrolineN-oxide, Dojindo, 1 mM) is used to capture OH and  $O_2^-$ , with the resultant (called spin trap adduct) of DMPO-OH. TEMPONE-H (1-Hydroxy-2,2,6,6-tetramethyl-4-oxo-piperidine, Enzo, 0.1 mM) is used to capture  $O_2^-$  and peroxyntirite (ONOO-/ONOOH) to generate the spin trap adduct TEMPONE.<sup>33</sup> Quantitative results of all ESR measurements are calibrated into absolute concentrations by using a stable radical, TEMPO. Each experiment is repeated three times.

### III. RESULTS AND DISCUSSIONS

#### A. Emission spectra of gaseous reactive species

The optical emission spectra of the two plasma jets are collected from the same position of the plasma plumes. The relative position of the fiber to the plasma jet devices is fixed (see Fig. 1). All optical diagnostics and power measurements are made with the water sample in place in order to keep the same conditions for the whole system. As shown in Fig. 2(a), the radiative species such as OH(A),  $N_2(C)$ ,  $N_2^+(B)$ , He( $3s^3S$ ), and O( $3p^5P$ ) have strong emission lines at 309, 337, 391, 706, and 777 nm, respectively.

According to Fig. 2(a), the emission intensity of  $N_2(C)$  and  $N_2^+(B)$  for the pulsed plasma jet is 1.8 times greater than that for the sinusoidal plasma jet. Besides, the emission intensity of He( $3s^3S$ ) of the pulsed plasma jet is about 1.2 times stronger than that of the sinusoidal plasma jet. However, the sinusoidal plasma jet is more efficient to produce more OH(A) and O( $3p^5P$ ). The emission intensity of OH(A) for the pulsed plasma jet is only about 20% of that for the sinusoidal plasma jet, and for O( $3p^5P$ ), it is about 60%. The result is somewhat different from the previous reports which have shown that the optical emission spectra of the pulsed plasma jet are stronger than that of the sinusoidal plasma jet for all the radiative species.<sup>15,27</sup> The difference between the previous reports and our work is that the

optical diagnostic measurements in our experiment are done with the water sample in place and the same discharge power for the two types of plasma jets. So, the reason for the phenomenon which the emission intensity of OH(A) and O( $3p^5P$ ) excited by sinusoidal plasma jet is higher than that of pulsed plasma jet might be that the sinusoidal plasma jet will release more heat to the liquid surface, prone to produce more water vapor to participate in the discharge, which promotes the generation of OH(A) and O( $3p^5P$ ) in the gas phase. Besides, the difference in the discharge characteristics which will lead to different distribution of high-energy electron density for the two types of plasma jets might be another reason.

For a small energy gap between rotational levels, the equilibrium between translational motion and rotational motion is readily achieved because of frequent collisions among heavy particles at atmospheric pressure; thus, the gas temperature of the plasma is approximately equal to the rotational temperature ( $T_{rot}$ ).<sup>28</sup> To determine the  $T_{rot}$  of the two types of plasma jets, the emission spectra of the OH( $A^2\Sigma \rightarrow X^2\Pi$ , 0-0) band are used to calculate the rotational temperature by comparing the experimental and simulation spectra using the LIFBASE software.<sup>29</sup> By comparing the best fitting simulation spectra to the experimental spectra shown in Figs. 2(b) and 2(c), gas temperature of the pulsed plasma jet is found to be lower than that of the sinusoidal plasma jet by  $\sim 20$  K. This result implies that the pulsed plasma jet converts more energy into reactive species, but the sinusoidal jet releases more energy for gas heating. The difference in gas temperature seems to be insignificant, but for biomedical applications, it might be important because the biological substance is sensitive to the gas temperature. For example, people may feel painful when the temperature at the epidermis–dermis interface is above 43 °C.<sup>31</sup> In this regard, the pulsed plasma jet can have a larger power density range, which facilitates the control of reactive species for biomedical applications.

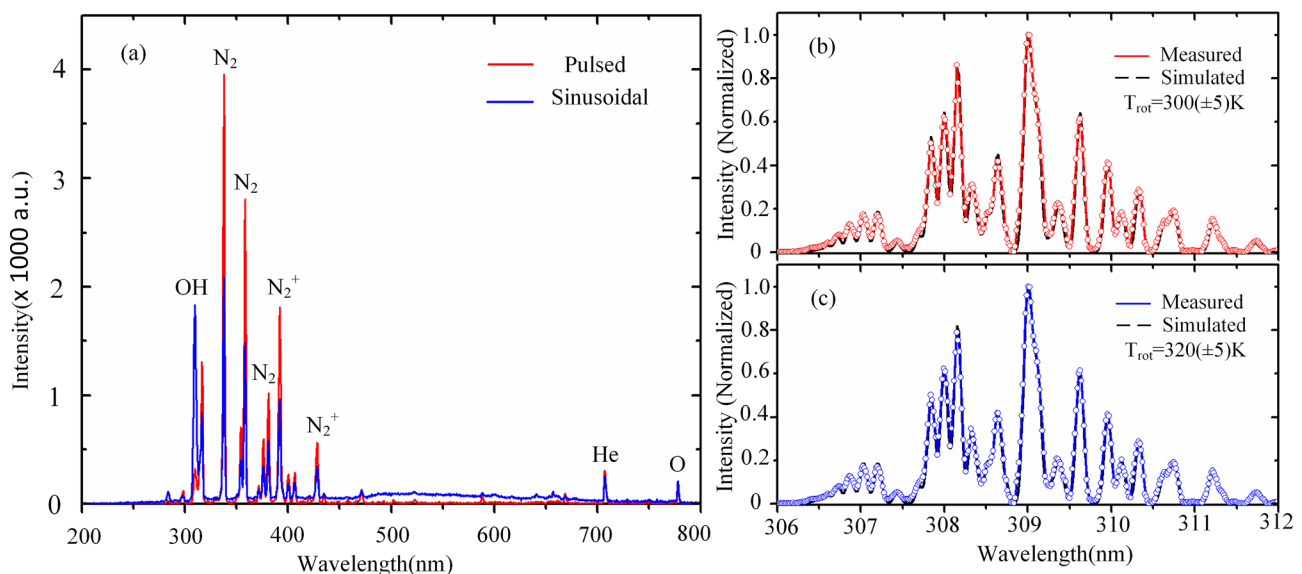


FIG. 2. Optical emission spectra in the range from 200 to 800 nm of the pulsed and sinusoidal helium plasma jets (a), the measured and simulated emission spectra of the OH band around 309 nm for the pulsed plasma jet (b) and sinusoidal plasma jet (c).

## B. Concentrations of aqueous reactive species

The concentrations of several aqueous RONS induced by the two types of plasma jets with the same discharge power of 700 mW are shown in Fig. 3. The concentration of spin adduct DMPO-OH reflects the concentrations of OH and  $O_2^-$ , and the spin adduct TEMPONE reflects the concentrations of  $O_2^-$  and ONOOH/ONOO $^-$ . The results demonstrate that the pulsed plasma jet can generate more aqueous reactive species than the sinusoidal one. Compared with the sinusoidal plasma jet, the aqueous  $H_2O_2$  for the pulsed plasma jet grows faster with the plasma treatment time, and the concentration difference between the two plasma jets gradually increases. As illustrated in Fig. 3(a), the concentration difference between the two jets is  $5.7 \mu\text{M}$  by 90 s, and it increases to  $12.3 \mu\text{M}$  by 180 s. According to our previous investigations,<sup>30,31</sup> these plasma produced  $H_2O_2$  in liquid can be generated through several chemical pathways. Besides, there are also studies that have shown that other important factors for the  $H_2O_2$  production are the processes taking place at the plasma–water interface, including sputtering, electric field induced hydrated ion emission, and evaporation.<sup>32</sup> Therefore the phenomenon that much more aqueous  $H_2O_2$  can be generated by the pulsed plasma jet than the sinusoidal plasma jet may be attributed to the larger particle fluxes of charged species and other short-lived species such as OH on the water.

For short-lived species, although the trapping reagents have been frequently reported for the measurement of OH and/or  $O_2^-$ , it should be noted that they might also react with other reactive species to produce the same spin adducts. For example, TEMPONE-H can react with peroxyxynitrite (ONOOH and ONOO $^-$ ) with a large rate coefficient of  $6 \times 10^9 \text{ M}^{-1} \text{ s}^{-1}$ , and the product is also TEMPONE.<sup>33</sup> So, the concentration of TEMPONE represents the total concentration of both  $O_2^-$  and peroxyxynitrite (ONOO-/ONOOH). Similarly, the trapping reagents DMPO can react with both OH and  $O_2^-$  to produce DMPO-OH, but the reaction with OH is much faster, and the DMPO will bind quicker with OH in presence of the same amount of OH and  $O_2^-$ ;<sup>34</sup> so, the results of DMPO-OH should mainly consist of the trapped OH radicals.

It can be seen from Figs. 3(b) and 4(c) that the concentrations of DMPO-OH and TEMPONE keep increasing with the treatment time for the two types of plasma jets. The concentration for the pulsed plasma jet is higher than that for the sinusoidal plasma jet for both of the spin adducts, but their differences are very small, less than  $2 \mu\text{M}$ , indicating that the concentrations of OH/ $O_2^-$  and  $O_2^-$ /ONOO $^-$  are similar for the two types of plasma jets. Although the concentration of DMPO-OH in liquid phase for the pulsed plasma jet is slightly larger than that for the sinusoidal plasma jet, the emission spectrum intensity of OH(A) for the pulsed plasma jet is weaker than the sinusoidal plasma jet; so, there is no significant correlation between them. According to recent reports by our group and others,<sup>30,31,35</sup> the main pathways for the production of aqueous OH include the solvation of gaseous OH, the VUV photo-dissociation of  $H_2O$  at the gas–liquid interface, and the liquid chemistry among some other species. For the aqueous  $O_2^-$ , the main production pathway is the electron attachment by the dissolved oxygen.

A further comparison of the concentrations of aqueous reactive species induced by sinusoidal and pulsed plasma jets is made by altering the discharge power from 570 to 820 mW. The growth trends of the concentrations along with the increasing discharge power are shown in Fig. 4. It can be seen that, for both long-lived reactive species  $H_2O_2$  and the adducts of short-lived species DMPO-OH and TEMPONE, their concentrations excited by the pulsed plasma jet increase faster than that by the sinusoidal plasma jet as a function of the discharge power. The concentration of  $H_2O_2$  increases from  $26.4 \mu\text{M}$  to  $40.2 \mu\text{M}$  as the discharge power increases from 570 mW to 820 mW for the pulsed plasma jet, while the concentration increases from  $18.6 \mu\text{M}$  to  $23.4 \mu\text{M}$  for the sinusoidal plasma jet. For the adduct DMPO-OH, the pulsed plasma jet also has a higher growth rate. The concentration of DMPO-OH increases  $22.4 \mu\text{M}$  with the discharge power from 570 mW to 820 mW for pulsed plasma jet, while  $12.8 \mu\text{M}$  for the sinusoidal plasma jet. The same phenomenon also applies for the adduct TEMPONE. The faster growth rates indicate that the discharge power is more efficiently consumed by producing reactive species for the

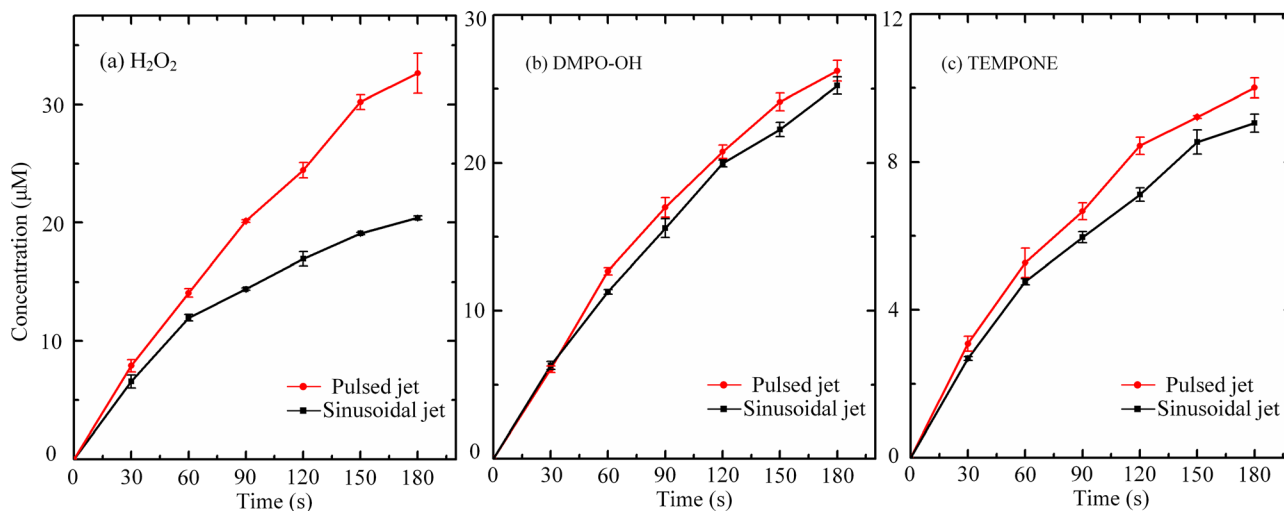


FIG. 3. Concentrations of  $H_2O_2$  (a), DMPO-OH (b), and TEMPONE (c) in the liquid phase as a function of the discharge treatment time for the two types of plasma jets with the power of 700 mW.

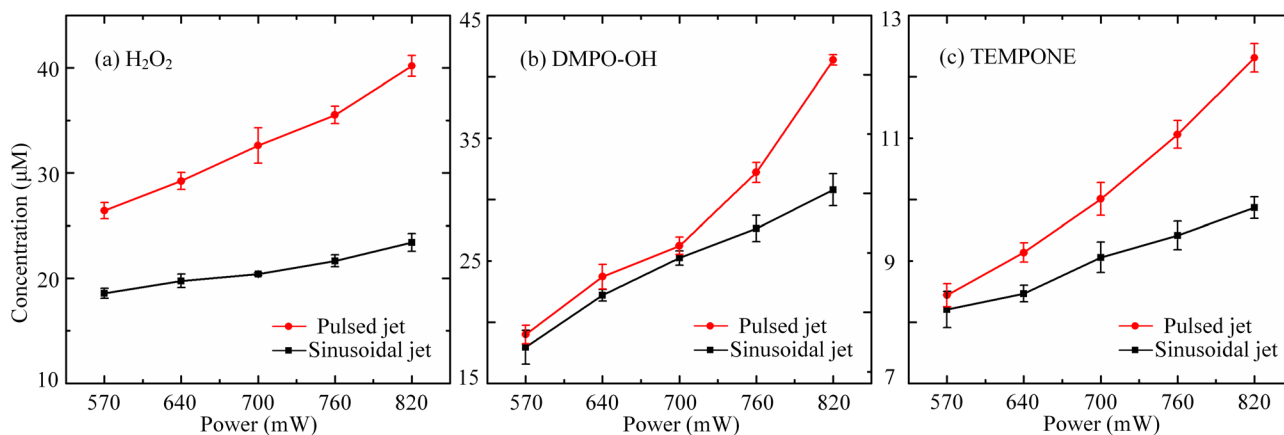


FIG. 4. Concentrations of H<sub>2</sub>O<sub>2</sub> (a), DMPO-OH (b), and TEMPONE (c) as a function of the discharge power for the two types of plasma jets. (The treatment time is 180 s.)

pulsed plasma jet. These results also demonstrate the effectiveness of regulating doses of reactive species by altering power supply of plasma jets, and are practical indicators to future application of using different types of plasma jets.

### C. Bacterial inactivation

To compare the bacterial inactivation effect of the two types of plasma jets, *Escherichia coli* (*E. coli*) is chosen for the plasma treatment. The bacterial samples are prepared in the following sequence. First, a bacterial culture with a concentration of about 10<sup>9</sup> CFU/ml (CFU: colony-forming unit) is prepared. Then, this bacterial culture is placed in an oven for an overnight incubation at 37 °C. After that, the bacterial culture is diluted to 10<sup>6</sup> CFU/ml. Finally, 2 mL of the bacterial samples on the petri dish is treated directly by the two types of plasma jets for 180 s. After the plasma treatment, the bacterial samples are diluted in different proportions and cultured on the agar plates, which are put back in the oven and incubated for 24 h at 37 °C. For the control experiments, the bacterial samples are treated using the same plasma

sources but without the applied voltage, i.e., the helium gas flow rate is the same but the plasma is off.

Figure 5 shows the bacterial inactivation results for the two types of plasma jets with respect to several discharge powers. It can be seen that the number of *E. coli* is decreased by more than one order of magnitude after being treated by the pulsed plasma jet at 570 mW, and the bacterial reduction increases to ~2 logs when the discharge power is 820 mW. In comparison, for the sinusoidal plasma jet, the bacterial reduction is much lower, and 820 mW of discharge power is needed to achieve ~1 log of reduction. Generally, the difference in the bacterial inactivation between the two types of plasma jets increases with the discharge power. The comparison between the bacterial inactivation results is in accordance with that for the concentrations of aqueous reactive species for the two types of plasma jets.

### IV. CONCLUSION

In conclusion, the water solutions treated by a pulsed plasma jet and a sinusoidal plasma jet with similar discharge power are comparatively studied, and the correlation

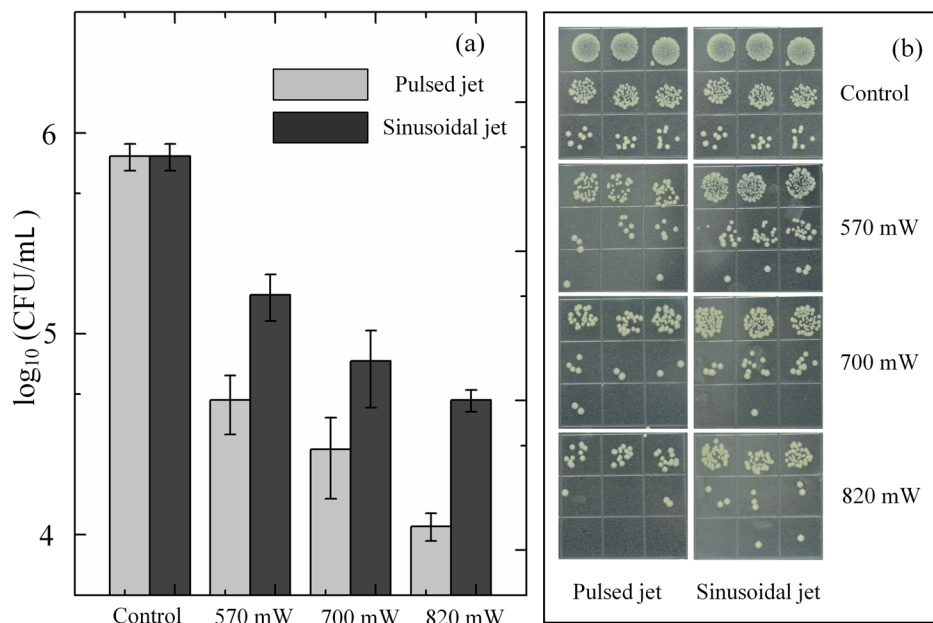


FIG. 5. The number of living *Escherichia coli* (a) and the corresponding photographs of bacterial samples on agar plates (b) as a function of the discharge power after being treated by the two types of plasma jets. The control group is also presented.

between gaseous and aqueous reactive species is discussed. It is found that the overall emission spectrum intensity for the pulsed plasma jet is stronger, but the emission intensities of OH(A) and O(3p<sup>5</sup>P) are lower due to the lower concentration of water vapor. This is because the gas temperature of the pulsed plasma jet is lower than that of the sinusoidal plasma jet, which hinders the evaporation of the plasma-treated water.

In the plasma-activated water, the aqueous H<sub>2</sub>O<sub>2</sub>, OH/O<sub>2</sub><sup>-</sup>, O<sub>2</sub><sup>-</sup>/ONOO<sup>-</sup> induced by the pulsed plasma jet have larger concentrations compared with that for the sinusoidal plasma jet, and the proportional differences in those concentrations increase with the discharge power. The result indicates that the discharge power is more efficiently consumed by producing reactive species for the pulsed plasma jet. In addition, the bacterial inactivation induced by the pulsed plasma jet is stronger than that for the sinusoidal plasma jet, in accordance with the concentration relation of aqueous RONS for the two types of plasma jets.

## ACKNOWLEDGMENTS

This work was supported by the National Science Foundation of China (Grant Nos. 51677147 and 51521065).

- <sup>1</sup>E. Stoffels, Y. Sakiyama, and D. B. Graves, *IEEE Trans. Plasma Sci.* **36**, 1441 (2008).
- <sup>2</sup>A. Shashurin, M. Keidar, S. Bronnikov, R. A. Jurjus, and M. A. Stepp, *Appl. Phys. Lett.* **93**, 181501 (2008).
- <sup>3</sup>X. Lu, G. V. Naidis, M. Laroussi, S. Reuter, D. B. Graves, and K. Ostrikov, *Phys. Rep.* **630**, 1–84 (2016).
- <sup>4</sup>M. Laroussi, *IEEE Trans. Plasma Sci.* **37**, 714 (2009).
- <sup>5</sup>K. D. Weltmann, E. Kindel, R. Brandenburg, C. Meyer, R. Bussiahn, C. Wilke, and T. von Woedtke, *Contrib. Plasma Phys.* **49**, 631 (2009).
- <sup>6</sup>G. Fridman, A. Shereshevsky, M. M. Jost, A. D. Brooks, A. Fridman, A. Gutsol, V. Vasilets, and G. Friedman, *Plasma Chem. Plasma Process.* **27**, 163 (2007).
- <sup>7</sup>G. C. Kim, G. J. Kim, S. R. Park, S. M. Jeon, H. J. Seo, F. Iza, and J. K. Lee, *J. Phys. D: Appl. Phys.* **42**, 032005 (2009).
- <sup>8</sup>H. J. Lee, C. H. Shon, Y. S. Kim, S. Kim, G. C. Kim, and M. G. Kong, *New J. Phys.* **11**, 115026 (2009).
- <sup>9</sup>Y. Li, M. H. Kang, H. S. Uhm, G. J. Lee, E. H. Choi, and I. Han, *Sci. Rep.* **7**, 45781 (2017).
- <sup>10</sup>M. Keidar and E. Robert, *Phys. Plasmas*. **22**, 121901 (2015).
- <sup>11</sup>S. Perni, W. Liu, G. Shama, and M. G. Kong, *J. Food Prot.* **71**, 302 (2008).
- <sup>12</sup>H. Xu, C. Chen, D. X. Liu, D. H. Xu, Z. J. Liu, X. H. Wang, and M. G. Kong, *J. Phys. D: Appl. Phys.* **50**, 245201 (2017).
- <sup>13</sup>A. Tani, Y. Ono, S. Fukui, S. Ikawa, and K. Kitano, *Appl. Phys. Lett.* **100**, 254103 (2012).
- <sup>14</sup>Z. J. Liu, D. H. Xu, D. X. Liu, Q. J. Cui, H. F. Cai, Q. S. Li, H. L. Chen, and M. G. Kong, *J. Phys. D: Appl. Phys.* **50**, 195204 (2017).
- <sup>15</sup>Q. Xiong, X. P. Lu, K. Ostrikov, Y. Xian, C. Zou, Z. Xiong, and Y. Pan, *Phys. Plasmas* **17**, 043506 (2010).
- <sup>16</sup>S. Wang, D. Z. Yang, W. C. Wang, S. Zhang, Z. J. Liu, K. Tang, and Y. Song, *Appl. Phys. Lett.* **103**, 264108 (2013).
- <sup>17</sup>X. J. Dai, C. S. Corr, S. B. Ponraj, M. Maniruzzaman, A. T. Ambujakshan, Z. Q. Chen, L. Kviz, R. Lovertt, G. D. Rajmohan, D. R. De celis, M. L. Wright, P. R. Lamb, Y. E. Krasik, D. B. Graves, W. G. Graham, R. d'Agostino, and X. G. Wang, *Plasma Process. Polym.* **13**, 306 (2016).
- <sup>18</sup>N. Shirai, S. Uchida, and F. Tochikubo, *Plasma Sources Sci. Technol.* **23**, 054010 (2014).
- <sup>19</sup>A. Lindsay, C. Anderson, E. Slikboer, S. Shannon, and D. B. Graves, *J. Phys. D: Appl. Phys.* **48**, 424007 (2015).
- <sup>20</sup>X. P. Lu, Z. H. Jiang, Q. Xiong, Z. Y. Tang, X. W. Hu, and Y. Pan, *Appl. Phys. Lett.* **92**, 081502 (2008).
- <sup>21</sup>F. Massines, A. Rabehi, P. Decomps, R. B. Gadri, P. Ségur, and C. Mayoux, *J. Appl. Phys.* **83**, 2950 (1998).
- <sup>22</sup>Z. Navrátil, R. Brandenburg, D. Trunec, A. Brablec, P. St'ahel, H. E. Wagner, and Z. Kopecký, *Plasma Sources Sci. Technol.* **15**, 8 (2006).
- <sup>23</sup>T. Nozaki, Y. Miyazaki, Y. Unno, and K. Okazaki, *J. Phys. D: Appl. Phys.* **34**, 3383 (2001).
- <sup>24</sup>M. Laroussi and T. Akan, *Plasma Process. Polym.* **4**, 777 (2007).
- <sup>25</sup>J. L. Walsh, J. J. Shi, and M. G. Kong, *Appl. Phys. Lett.* **88**, 171501 (2006).
- <sup>26</sup>A. Mizuno, J. S. Clements, and R. H. Davis, *IEEE Trans. Ind. Appl. IA-* **22**, 516 (1986).
- <sup>27</sup>S. Zhang, W. C. Wang, P. C. Jiang, D. Z. Yang, L. Jia, and S. Wang, *J. Appl. Phys.* **114**, 163301 (2013).
- <sup>28</sup>S. Q. Luo, C. M. Denning, and J. E. Scharer, *J. Appl. Phys.* **104**, 013301 (2008).
- <sup>29</sup>J. Luge and D. R. Crosley, SRI International Report No. MP 99-009 (1999).
- <sup>30</sup>D. X. Liu, Z. C. Liu, C. Chen, A. J. Yang, D. Li, M. Z. Rong, H. L. Chen, and M. G. Kong, *Sci. Rep.* **6**, 23737 (2016).
- <sup>31</sup>C. Chen, D. X. Liu, Z. C. Liu, A. J. Yang, H. L. Chen, G. Shama, and M. G. Kong, *Plasma Chem. Plasma Process.* **34**, 403 (2014).
- <sup>32</sup>J. D. Liu, B. B. He, Q. Chen, J. S. Li, Q. Xiong, G. H. Yue, X. H. Zhang, S. Z. Yang, H. Liu, and Q. H. Liu, *Sci. Rep.* **6**, 38454 (2016).
- <sup>33</sup>S. Dikalov, M. Skatchkov, and E. Bassenge, *Biochem. Bioph. Res. Commun.* **230**, 54–57 (1997).
- <sup>34</sup>H. Tresp, M. U. Hammer, K. D. Weltmann, and S. Reuter, *J. Phys. D: Appl. Phys.* **46**, 435401 (2013).
- <sup>35</sup>W. Tian and M. J. Kushner, *J. Phys. D: Appl. Phys.* **47**, 165201 (2014).